Supporting Information

Johnson et al. 10.1073/pnas.1219578110

SI Materials and Methods

Electrophysiology. Apical inner hair cells (IHCs) in mice overexpressing SK2 channels (SK2 +/T: OE) and their control littermates (+/+) were studied in acutely dissected organs of Corti from postnatal day 1 (P1) to P27. The cochleae were dissected as previously described (1) in the following solution (in mM): 135 NaCl, 5.8 KCl, 1.3 $CaCl_2$, 0.9 $MgCl_2$, 0.7 NaH_2PO_4, 5.6 D-glucose, 10 Hepes–NaOH, 2 Na pyruvate, amino acids, and vitamins (pH 7.5; osmolality ~308 mmol·kg^{-1}). The dissected cochleae were transferred to a microscope chamber, immobilized under a nylon mesh attached to a stainless steel ring, and continuously perfused with a peristaltic pump using the above extracellular solution. The isolated SK2 current was obtained by subtracting the current in the presence of a Ca^{2+}-free solution containing 0.5 mM EGTA from the total K^+ current.

Electrophysiological recordings were made using the Optopatch (Cairn Research Ltd) amplifier. Data acquisition was controlled by pClamp software using the Digidata 1440A interface (Molecular Devices). Data analysis was performed with Origin (Origin Lab). The Mini Analysis Program (Synaptosoft Inc.) was used to detect action potentials in whole-cell and biphasic spike events in the cell-attached configuration, to calculate their frequency, and to analyze interspike intervals (ISIs) and amplitudes. The action potential frequency was calculated as the reciprocal of the mean ISI for each cell, and an indication of the spread of ISI values about the mean was obtained by calculating the coefficient of variation, equal to the SD divided by the mean (2).

Patch pipettes were made from Soda glass capillaries (Harvard Apparatus Ltd) and coated with surf wax (SexWax, M_r Zoggs) to minimize the fast transients due to the patch pipette capacitance. For whole-cell recordings, soda glass pipettes were filled with (in mM): 131 KCl, 3 $MgCl_2$, 1 EGTA–KOH, 5 Na_2ATP, 5 Hepes–KOH, and 10 Na_2-phosphocreatine (pH 7.3; osmolality ~296 mmol kg^{-1}). For cell-attached recordings the pipette solution was (in mM): 140 NaCl, 5.8 KCl, 1.3 $CaCl_2$, 0.9 $MgCl_2$, 0.7 NaH_2PO_4, 5.6 D-glucose, 10 Hepes-NaOH (pH 7.5; osmolality ~294 mmol·kg^{-1}). The intracellular solution used for exocytosis measurements contained (in mM): 106 Cs-glutamate, 20 CsCl, 3 $MgCl_2$, 1 EGTA–CsOH, 5 Na_2ATP, 0.3 Na_2GTP, 5 Hepes–CsOH, 10 Na_2–phosphocreatine (pH 7.3; osmolality ~296 mmol·kg^{-1}). Real-time changes in membrane capacitance (ΔC_m) were measured as previously described (3,4). Briefly, ΔC_m was measured using a 4 kHz sine wave (13 mV rms) applied to hair cells from a holding potential of −81 mV and was interrupted for the duration of the voltage step. The capacitance signal from the Optopatch was amplified (×50), filtered at 250 Hz, sampled at 5 kHz, and measured by averaging the C_m traces after the voltage step (around 200 ms) and subtracting from prepulse baseline. ΔC_m was recorded in the presence of K^+ channel blockers TEA (30 mM), 4-AP (15 mM), and linopirdine (80–100 μM). Membrane potentials were corrected for the voltage drop across the series resistance R_s and a liquid junction potential of –4 mV (KCl-based intracellular solution) or –11 mV (Cs-glutamate–based solution).

Statistical Analysis. Statistical comparisons of means were made by Student's two-tailed t test or, for multiple comparisons, one- or two-way ANOVA followed by the Tukey or Bonferroni test, respectively. Means are quoted ± SEM, and $P < 0.05$ was used as the criterion for statistical significance.

Immunofluorescence Labeling. Cochleae from immature and adult mice were used to prepare cryosections for immuno-fluorescence microscopy and processed as previously described (5,6). Briefly, cochleae were fixed for 2 h with 2% paraformaldehyde (wt/vol), embedded in Tissue-Tek, and cryosectioned at a thickness of 10 μm. Antibodies to SK2 channels (rabbit, Sigma, diluted 1:50), otoferlin (mouse, monoclonal, Abcam, diluted 1:50), $Ca_V1.3$ (rabbit, Alomone Laboratories, diluted 1:50), and CtBP2/Ribeye (mouse, BD Transduction Laboratories, diluted 1:50) were used. Primary antibodies were detected with Cy3-conjugated (Jackson ImmunoResearch Laboratories) or Alexa Fluor 488–conjugated secondary antibodies (Molecular Probes). Cochlea sections were imaged and analyzed as previously described (4). Sections were viewed using an Olympus BX61 microscope equipped with motorized z axis and epifluorescence illumination. Images were acquired using a CCD camera and analyzed with cellSens Dimension software (Olympus soft imaging solutions, OSIS). To display SK2 channel distribution, cochlea slices were imaged over a distance of several μm to cover the IHC width in an image stack along the z-axis (z stack) followed by 3D deconvolution (cellSense Dimensions, OSIS). Immunostaining pictures show composite images, which represent the maximum intensity projection over all layers of the z stack.

Transmission Electron Microscopy. For transmission electron microscopy, cochleae were perfused with 2.5% (vol/vol) glutaraldehyde in 0.1 M sodium cacodylate/2 mM calcium chloride buffer through the round window, immersed in fixative for 2 h, and then stored in the buffer. The cochleae were partially dissected and postfixed in 1% osmium tetroxide in cacodylate buffer for 1 h, dehydrated through an ethanol series, and embedded in Spurr resin via 1:1 and 3:1 resin ethanol intermediate stages and then in pure resin three times before polymerization of the resin at 60 °C for 16 h (7). Radial and horizontal ultrathin sections were taken of the apical turns, stained in 2% (wt/vol) ethanolic uranyl acetate and 2% (wt/vol) aqueous lead citrate, and examined in a JEOL 100CX or JEOL 100S transmission electron microscope at 80 or 100 kV, respectively. Images were acquired using Megaview III or a custom-made digital camera system.

1. Marcotti W, Johnson SL, Holley MC, Kros CJ (2003) Developmental changes in the expression of potassium currents of embryonic, neonatal and mature mouse inner hair cells. *J Physiol* 548(Pt 2):383–400.
2. Johnson SL, et al. (2011) Position-dependent patterning of spontaneous action potentials in immature cochlear inner hair cells. *Nat Neurosci* 14(6):711–717.
3. Johnson SL, Forge A, Knipper M, Münkner S, Marcotti W (2008) Tonotopic variation in the calcium dependence of neurotransmitter release and vesicle pool replenishment at mammalian auditory ribbon synapses. *J Neurosci* 28(30):7670–7678.
4. Johnson SL, et al. (2010) Synaptotagmin IV determines the linear Ca^{2+} dependence of vesicle fusion at auditory ribbon synapses. *Nat Neurosci* 13(1):45–52.
5. Heidrych P, et al. (2009) Otoferlin interacts with myosin VI: Implications for maintenance of the basolateral synaptic structure of the inner hair cell. *Hum Mol Genet* 18(15):2779–2790.
6. Knipper M, et al. (2000) Thyroid hormone deficiency before the onset of hearing causes irreversible damage to peripheral and central auditory systems. *J Neurophysiol* 83(5):3101–3112.
7. Furness DN, Hackney CM (1985) Cross-links between stereocilia in the guinea pig cochlea. *Hear Res* 18(2):177–188.
8. Guinan JJ, Jr. (1996) Physiology of olivocochlear efferents. *The Cochlea*, eds Dallos P, Popper AN, Fay RR (Springer, New York), pp 435–502.
9. Pujol R, Lavigne-Rebillard M, Lenoir M (1998) Development of sensory and neural structures in the mammalian cochlea. *Development of the Auditory System*, eds Rubel EW, Popper AN, Fay RR (Springer, New York), pp 146–192.
10. Glowatzki E, Fuchs PA (2000) Cholinergic synaptic inhibition of inner hair cells in the neonatal mammalian cochlea. *Science* 288(5475):2366–2368.

11. Katz E, et al. (2004) Developmental regulation of nicotinic synapses on cochlear inner hair cells. *J Neurosci* 24(36):7814–7820.
12. Marcotti W, Johnson SL, Kros CJ (2004) A transiently expressed SK current sustains and modulates action potential activity in immature mouse inner hair cells. *J Physiol* 557(Pt 2):613–633.
13. Kros CJ, Ruppersberg JP, Rüsch A (1998) Expression of a potassium current in inner hair cells during development of hearing in mice. *Nature* 394(6690): 281–284.

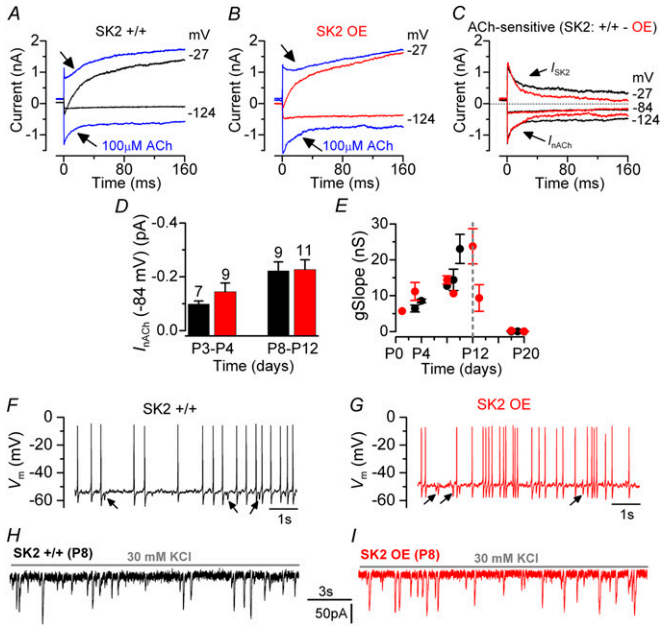

Fig. S1. Efferent modulation of control and OE SK2 IHCs. The olivocochlear efferent fibers of the auditory nerve exert an inhibitory role on hair cell activity by releasing the neurotransmitter acetylcholine (ACh). In the mature animal, the principal targets of efferent fibers are OHCs (1). However, during immature development, efferent endings make transient axosomatic synaptic contacts with IHCs (2). Adult IHCs no longer respond to ACh (3) since the few remaining efferent fibers found below mature IHCs make axodendritic contacts with the afferent fibers (2). In immature IHCs, the ACh-activated current, which is mediated by Ca^{2+} entering hair cells through α9α10-nicotinic ACh receptors (nAChRs) that activates SK2 channels, is initially detected in apical IHCs from just after birth up to around P15–P16 (4,5). This efferent fiber-induced SK2 current is inhibitory and causes IHCs to hyperpolarize (3,5). (*A–C*) Membrane currents were recorded from control ($^{+/+}$, black) and SK2 OE (red) immature P8 IHCs before and during (blue traces) extracellular application of 100 μM ACh. In the presence of ACh, depolarizing and hyperpolarizing voltage steps from the holding potential of −64 mV elicited an instantaneous current (arrows), which is carried by SK2 channels and nAChRs (5), in all IHCs. The isolated ACh-sensitive currents for both control and SK2 OE cells (*C*) were obtained by subtracting the current obtained without ACh (control: black lines in *A*; SK2 OE, red lines in *B*) from that in the presence of ACh (blue lines in *A* and *B*). A similar method has previously been used to study the developmental expression of the ACh-activated current in wild-type mice (5). The outward component at more depolarized potentials is mainly carried by the SK2 channels, whereas the inward current when the cell is hyperpolarized predominantly flows through the nAChRs (5). (*D*) Size of the steady-state inward ACh-sensitive current available at −84 mV (see panel *C* for an example at P8) (5) in P3–P4 and P8–P12 IHCs from control and SK2 OE mice. We found that the current measured at −84 mV, which would mainly be that going through the nAChRs since at this voltage there would be little driving force for K^+ movement through SK2 channels, was not significantly different between control and SK2 OE IHCs. (*E*) Developmental change in the steady-state slope conductance measured near −84 mV in the presence of 100 μM ACh (number of IHCs tested for controls: 5, 2, 1, 4, 4, 4, 6, 3; SK2 OE: 1, 5, 3, 1, 4, 3, 2, 2). Note that both control (black) and SK2 OE (red) IHCs showed similar responses to ACh and were no longer sensitive to the neurotransmitter by P18–P20, as previously described (3,5). Although two-way ANOVA could not be performed because of the limited amount of overlapping days tested for both genotypes, *t* tests for the overlapping points showed no significant difference. The similar ACh responses, despite the larger SK2 current in OE IHCs, indicate that the additional SK2 channels were not colocalized with α9α10-nicotinic receptors (5). (*F* and *G*) Spontaneous action potentials recorded using whole-cell current clamp at body temperature from control (*F*) and SK2 OE (*G*) immature IHCs. Note that hyperpolarizing potentials (some indicated by arrows), which represent the inhibitory postsynaptic potentials (IPSPs) mediated by the spontaneous release of ACh from efferent fibers, are present in both control and OE IHCs. The size of spontaneous IPSPs in control and SK2 OE IHCs were not significantly different between control (6.59 ± 0.16 mV, $n = 60$ from 8 IHCs) and SK2 OE (6.60 ± 0.19 mV, $n = 47$ from 7 IHCs) mice. (*H* and *I*) To measure evoked release of ACh from efferent fibers, IHCs were voltage clamped at −84 mV and inhibitory postsynaptic currents (IPSCs) were elicited by depolarizing the efferent terminals with an extracellular solution containing 30 mM KCl (gray lines above the traces). The size of evoked IPSCs was also not significantly different between control and SK2 OE IHCs (control, 68.3 ± 7.9 pA, $n = 2,018$ from 5 IHCs; SK2 OE, 63.1 ± 3.5 mV, $n = 6,397$ from 15 IHCs). These results indicate that the overexpression of SK2 channels does not influence the biophysical properties and development of the efferent system.

1. Guinan JJ, Jr. (1996) Physiology of olivocochlear efferents. *The Cochlea*, eds Dallos P, Popper AN, Fay RR (Springer, New York), pp 435–502.
2. Pujol R, Lavigne-Rebillard M, Lenoir M (1998) Development of sensory and neural structures in the mammalian cochlea. *Development of the Auditory System*, eds Rubel EW, Popper AN, Fay RR (Springer, New York), pp 146–192.
3. Glowatzki E, Fuchs PA (2000) Cholinergic synaptic inhibition of inner hair cells in the neonatal mammalian cochlea. *Science* 288(5475):2366–2368.
4. Katz E, et al. (2004) Developmental regulation of nicotinic synapses on cochlear inner hair cells. *J Neurosci* 24(36):7814–7820.
5. Marcotti W, Johnson SL, Kros CJ (2004) A transiently expressed SK current sustains and modulates action potential activity in immature mouse inner hair cells. *J Physiol* 557(Pt 2): 613–633.

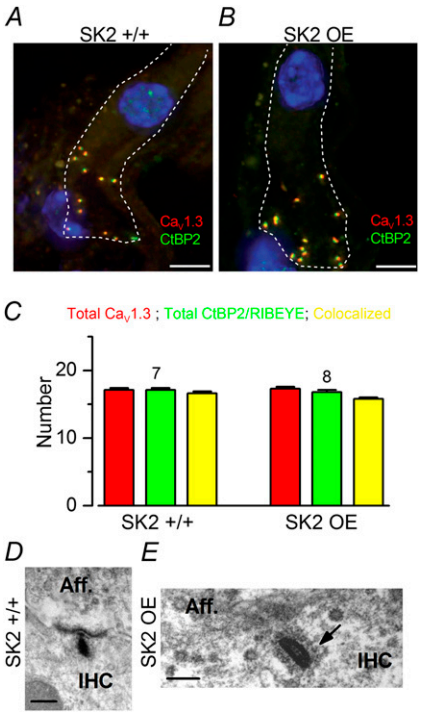

Fig. S2. Morphology of ribbon synapses in SK2 OE IHCs. (*A* and *B*) Merged images showing the distribution of synaptic ribbons (CtBP2/RIBEYE, green) and $Ca_V1.3$ channels (red) within apical IHCs from control (*A*) and SK2 OE (*B*) mice. Note that both $Ca_V1.3$ Ca^{2+} channels and ribbons are localized at the synaptic region of IHCs. Images show colocalization between CtBP2/RIBEYE and Ca^{2+} channel immunopositive spots in yellow. White dotted lines delineate IHCs. Images represent the maximum intensity projection over all layers of the z-stack. Nuclei were stained with DAPI (blue). (Scale bar, 5 μm.) (*C*) Total number of immunopositive spots for $Ca_V1.3$ (red bar), total number of CtBP2/RIBEYE (green bar), and total number of colocalized (yellow bar) were not significantly different between control and SK2 OE IHCs. Number of IHCs analyzed is indicated above the bars. (*D* and *E*) Transmission electron microscopy showing the cross-sectional profiles of presynaptic dense bodies (ribbons) from a control and an OE adult P22 IHC, respectively. aff, afferent endings. (Scale bar, 200 nm.) The height of synaptic ribbons in adult SK2 OE IHCs (244 ± 15 nm, $n = 10$ ribbons) was not significantly different to that measured in control cells (292 ± 25 nm, $n = 10$ ribbons) or previously reported in mature mouse IHCs (1).

1. Johnson SL, et al. (2010) Synaptotagmin IV determines the linear Ca^{2+} dependence of vesicle fusion at auditory ribbon synapses. *Nat Neurosci* 13(1):45–52.

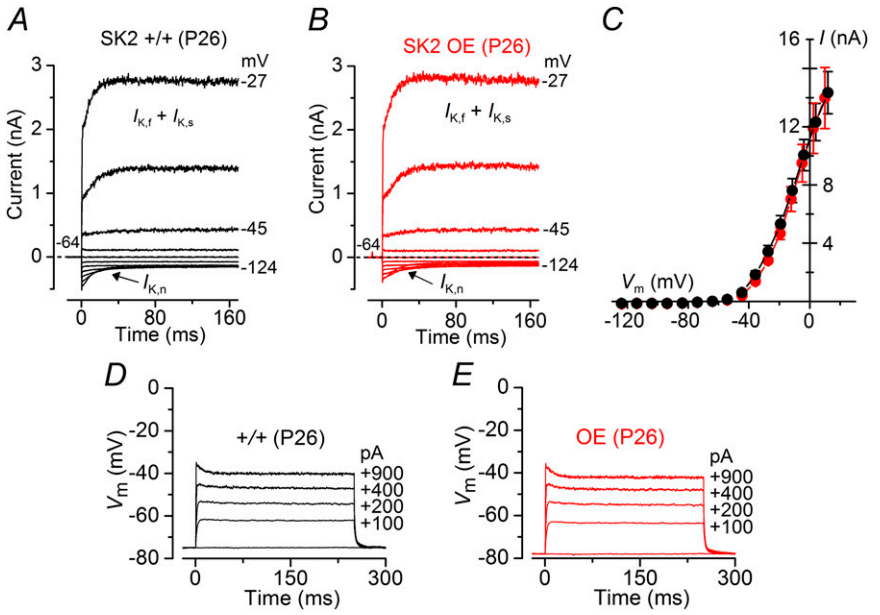

Fig. S3. Potassium currents in control and SK2 OE IHCs. (*A* and *B*) Potassium currents recorded from a control (+/+) and an SK2 OE adult P26 IHC, respectively. Membrane currents were elicited in response to depolarizing voltage steps in 10 mV increments from –124 mV (holding potential –64 mV) to the various test potentials shown by some of the traces. Note the control and OE IHCs express the same K^+ currents: I_K (1), $I_{K,f}$ (2), and $I_{K,n}$ (1) (Table 1). (*C*) Average total K^+ current–voltage relation for the control ($n = 3$) and OE ($n = 4$) IHCs. (*D* and *E*) Voltage responses under whole-cell current clamp in control (*D*) and OE (*E*) P26 IHCs. Responses were elicited by applying depolarizing current injections in 100 pA increments from the IHC resting membrane potential. For clarity, only a few voltage responses are shown.

1. Marcotti W, Johnson SL, Holley MC, Kros CJ (2003) Developmental changes in the expression of potassium currents of embryonic, neonatal and mature mouse inner hair cells. *J Physiol* 548(Pt 2):383–400.
2. Kros CJ, Ruppersberg JP, Rüsch A (1998) Expression of a potassium current in inner hair cells during development of hearing in mice. *Nature* 394(6690):281–284.